Monte Carlo and integral-equation studies of hard-oblate-spherocylinder fluids

J. Šedlbauer,* S. Labík, and A. Malijevský
Department of Physical Chemistry, Prague Institute of Chemical Technology, Prague 166 28, Czech Republic
(Received 24 November 1993)

Hard-oblate spherocylinders with reduced core diameters $l^* = l/\sigma = 1, 2, 3$ are studied at several packing fractions up to $\eta = 0.45$. Monte Carlo results are given for the first six spherical harmonic coefficients of the pair distribution function, $g_{k\ell m}(r)$, and for the compressibility factors. These results are compared with the hypernetted chain (HNC), Percus-Yevick (PY), and modified Verlet (VM) approximations. The VM theory produces very good results for the g_{000} harmonic coefficient at low and medium densities and for the reduced coefficients $g^*_{k\ell m} = g_{k\ell m}/g_{000}$ at all densities considered. The PY and HNC results are less accurate and none of the theories satisfactorily describes the g_{000} harmonic coefficient at $\eta = 0.45$. The VM theory gives equation-of-state results in excellent agreement with the simulation data, whereas the PY values of the compressibility factors at medium and high densities are too low while the HNC values are too high. The thermodynamic consistency between the pressure and the compressibility equations is also tested for each of the PY, HNC, and VM theories. At all state points considered the consistency of the VM theory is much better than that of the PY and HNC theories. Finally, we report results for the first bridge diagram (the first term in the density expansion of the bridge function) at several specific orientations of the root molecules.

PACS number(s): 61.25.Em

I. INTRODUCTION

The hard spherocylinder fluid is a popular model in studying fluid structure and thermodynamics because hard-prolate-spherocylinders (HPS) and hard-oblate-spherocylinders (HOS) capture some properties of real fluids of rodlike and disk-shaped molecules, respectively. HPS fluids have been often studied whereas computer simulation and theoretical results for HOS fluids are rather scarce. Several authors calculated virial coefficients [1,2]. Besides these low density results we are aware of no studies of the HOS system except the work of Wojcik and Gubbins [2] who reported Monte Carlo structural and equation-of-state data. The reason for this discrimination against HOS systems is rather technical than physical; it is easier to calculate particle-particle distance of prolate than of oblate hard spherocylinders.

The HOS model is characterized by the reduce core diameter $l^* = l/\sigma$ where l is the diameter of the disk core and σ is the thickness of the spherocylinder (for hard spheres, $l = 0$). The second parameter characterizing the model is the packing fraction η, the fraction of volume occupied by spherocylinders, given by $\eta = \rho v$, where ρ is the particle number density and $v = (6l^{*2} + 3\pi l^* + 4)\pi\sigma^3/24$ is the oblate spherocylinder volume.

There are three aims of this paper. First, we provide Monte Carlo (MC) computer simulation results for the compressibility factors and for the spherical harmonic coefficients of the pair distribution function $g(12)$. Second, we compare the MC data with the results of the Percus-Yevick (PY), hypernetted chain (HNC), and modified Verlet (VM) [3] theories. Third, we calculate, using Monte Carlo integration, the first bridge diagram at several specific orientations and distances of the root particles.

II. MONTE CARLO SIMULATIONS

We performed several Monte Carlo simulations using standard Metropolis procedure with a cubic box and periodic boundary conditions. Technical details of the simulations, including evaluation of the compressibility factor, $z = \beta P/\rho$, were similar to those of Wojcik and Gubbins [2]. A number of molecules in the box was maintained in the range 500–540 in the dependence on l^*. We started from a regular lattice at the highest densities and from the nearest higher density at lower densities. After equilibration, approximately 3×10^6–5×10^6 trial configurations were generated. Statistical error of results was estimated by a method of subaverages. We collected values necessary for determining the compressibility factors [1] and six harmonic coefficients of the pair distribution function, $g(12)$ in the center-center molecular coordinate frame. We considered the coefficients $g_{000}(r)$, $g^*_{200}(r)$, $g^*_{220}(r)$, $g^*_{221}(r)$, $g^*_{222}(r)$, and $g^*_{400}(r)$, where $g^*_{klm}(r) = g_{klm}(r)/g_{000}(r)$ are reduced harmonic coefficients.

III. ORNSTEIN-ZERNIKE EQUATION THEORIES

The Ornstein-Zernike (OZ) equation relates the direct correlation function $c(12)$ and the total correlation func-

*Mailing address: Department of Physical Chemistry, Prague Institute of Chemical Technology, 166 28 Praha 6, Czech Republic. Electronic address: josef.sedlbauer@vscht.cz

tion, $h(12) = g(12) - 1$,

$$h(12) = c(12) + \rho \int h(13)c(32)\, d(3)\,. \tag{1}$$

It is convenient to write the discontinuous functions h and c in terms of smooth functions, the series function γ, and the bridge function B:

$$h(12) = \exp[-\beta u(12) + \gamma(12) - B(12)] - 1\,, \tag{2}$$

$$c(12) = h(12) - \gamma(12)\,, \tag{3}$$

where $u(12)$ is the interparticle pair potential (for hard bodies it is infinite when two particles overlap and zero otherwise), and $\beta = 1/(k_B T)$.

The OZ equation may be closed by postulating a relation between the series and the bridge functions. The closures considered in this work are the PY closure

$$B(12) = \gamma(12) - \ln[1 + \gamma(12)]\,, \tag{4}$$

the HNC closure

$$B(12) = 0\,, \tag{5}$$

and the VM closure [3]

$$B(12) = \frac{1}{2}\,\frac{\gamma(12)^2}{1 + (1.1 - 2\eta/\pi)\gamma(12)}\,. \tag{6}$$

The numerical algorithm of solving the OZ equation is similar to that used in our previous papers [3–5] and is described in detail in a separate paper [6]. It consists of expanding the correlation functions in spherical harmonics in the center-center frame, discretizing them, transforming to Fourier space, and solving the resulting set of nonlinear equations by an approximate Newton-Raphson method. We carried out the numerical calculations using $N = 512$ grid points with the step size in configuration space being $\Delta r = 0.01$. We used 14 spherical harmonics $X_{k\ell m}$ with k, $\ell = 0, 2, 4$ and $m = 0, \ldots, 4$.

The compressibility factor, z, may be calculated from the pressure equation, which for the hard bodies gives

$$z = 1 + \frac{2}{3}\pi\rho\langle r^3 g(12)\rangle\,, \tag{7}$$

where $\langle\,\rangle$ denotes the angular average of $r^3 g(12)$ when two molecules are in contact. The alternative route to the equation of state is via the compressibility equation

$$\beta\left(\frac{\partial P}{\partial \rho}\right)_\beta = \left[1 + 4\pi\rho\int_0^\infty h_{000}(r) r^2 dr\right]^{-1} = 1 - 4\pi\rho\int_0^\infty c_{000}(r) r^2 dr\,. \tag{8}$$

IV. THE FIRST BRIDGE DIAGRAM

In the low density limit the series and the bridge function become

$$\gamma(12) = \rho D_1(12)\,, \tag{9}$$

$$B(12) = \frac{1}{2}\rho^2 D_2(12) \tag{10}$$

where

$D_1(12) =$ 

and

$D_2(12) = -$  .

We calculated $D_1(12)$ and $D_2(12)$ using Monte Carlo integration. The first series diagram may be written as

$$D_1(12) = P_1(12) V(12)\,, \tag{11}$$

where $P_1(12)$ is a probability that the field particle 3, randomly placed into the space element of volume $V(12)$ is overlapping with the fixed root particles 1 and 2. For each considered distance and orientation of the root particles we used 10^6 trial configurations of particle 3 to calculate $P_1(12)$. Configurations at which particles formed a chain (i.e., particle 3 overlapped with 1 and 2) were stored and used to calculate $D_2(12)$.

The first bridge diagram may be written as

$$D_2(12) = D_1^2(12) P_2(12)\,, \tag{12}$$

where $P_2(12)$ is a probability that field particles of two accidentally chosen three-member chains overlap. To evaluate $P_2(12)$ first 1024 chains

obtained and stored as mentioned above were used; each pair of the chains was tested on overlapping of the field particles. The series and bridge diagrams were calculated for four specific orientations of root spherocylinders, plane, T-shape, cross, and parallel (see Fig. 3), at several distances ranging from contact distance r_c to the distance $r = r_c + l + \sigma$ at which $D_2(12)$ vanishes.

V. RESULTS AND DISCUSSION

Monte Carlo simulations were carried out for three reduced core diameters $l^* = 1, 2, 3$ at three packing fractions $\eta = 0.25, 0.35, 0.45$. We solved the OZ equation for the same values of l^* at eight packing fractions ranging from 0.05 to 0.45.

The OZ equation theories provide uniformly excellent results in the low density region. At high densities the VM theory values of $g_{k\ell m}(r)$ are within the precision of the simulations for the reduced core diameter $l^* = 1$. This is not surprising. The VM theory gives accurate results for hard spheres ($l^* = 0$) in the entire fluid density range [3] and, thus, it must be excellent at low core diameters and all fluid densities. At this core diameter and high densities the PY theory slightly overestimates and the HNC theory slightly underestimates the extremes of $g_{000}(r)$ harmonic coefficient but, generally, their structure results are also very good.

In Figs. 1 and 2 we show the structure results of the

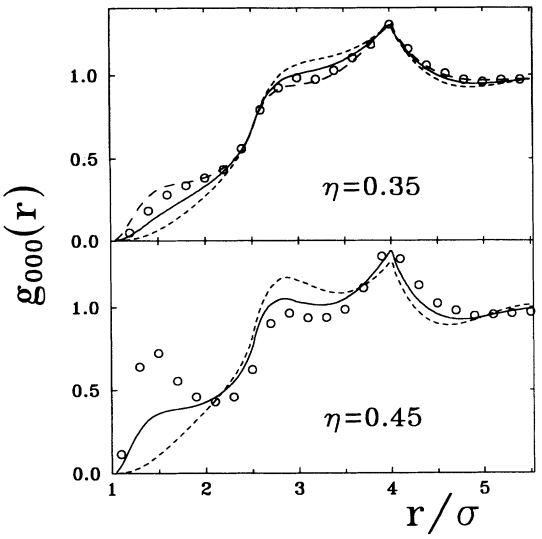

FIG. 1. g_{000}, the harmonic coefficient of the pair distribution function at $l^* = 3$ and at $\eta = 0.35$ and 0.45. ○, Monte Carlo data; – – – PY theory; — — — HNC theory; ——— VM theory.

PY, HNC, and VM theories for the largest core diameter at the highest densities. Figure 1 compares the theoretical results for $g_{000}(r)$ with our computer simulation results at $l^* = 3$ and $\eta = 0.35$ and 0.45. At the lower density the HNC results are the best and the PY results the worst. The VM theory underestimates the simulation results in the contact region and gives good results at larger interparticle distances. At the highest density considered, $\eta = 0.45$, the PY and VM results are poor.

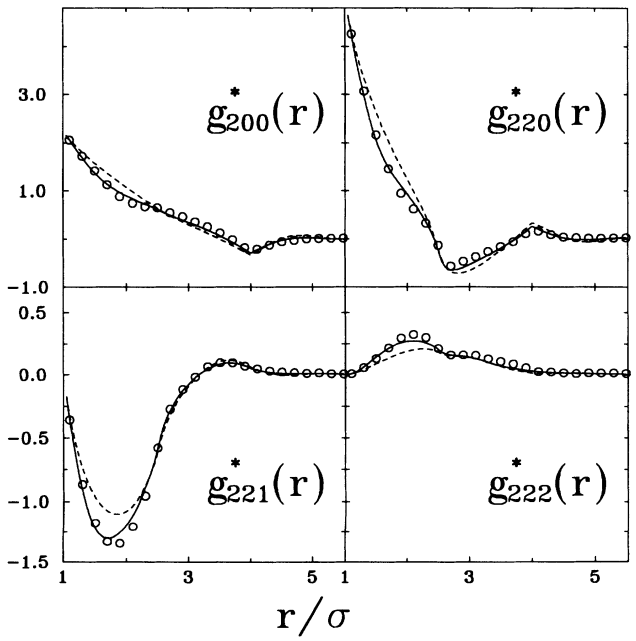

FIG. 2. g_{2lm} reduced spherical harmonic coefficients of the pair distribution function at $l^* = 3$ and $\eta = 0.45$. The key is the same as Fig. 1.

Numerical solution to the HNC equation could not be obtained.

Figure 2 shows the reduced spherical harmonic coefficients g^*_{200}, g^*_{220}, g^*_{221}, and g^*_{222} for $l^* = 3$ and $\eta = 0.45$. The VM theory gives excellent results; the PY harmonic coefficients are in a reasonable agreement with the simulation data. This indicates that the main discrepancies of the theories considered are in the leading harmonic coefficient $g_{000}(r)$.

Table I compares the PY, HNC, and VM compressibility factors calculated from the pressure equation (7) with Wojcik and Gubbins [2] and present MC results and with the results of a semiempirical equation of state recently proposed by Maeso, Solana, and Amoros [7]. The two simulation data sets mutually agree within estimated errors (see columns 2 and 3). The results of the equation of state (column 3) agree with the MC data within the precision of the simulations at all but one state point ($l^* = 3$, $\eta = 0.45$). The VM compressibility factors are very good. The PY and HNC results are consistently too low and too high, respectively.

We have tested the thermodynamic consistency of the theories by comparing the compressibility factors from the pressure equation (7) and the compressibility equation (8). The latter were calculated by the same method as in Ref. [5]. The results are shown in Table II. It is seen that the consistency of the VM theory is much better than that of the PY and the HNC theories.

The first bridge diagrams $D_2(12)$ for several orientations and all elongations are displayed in Fig. 3 together

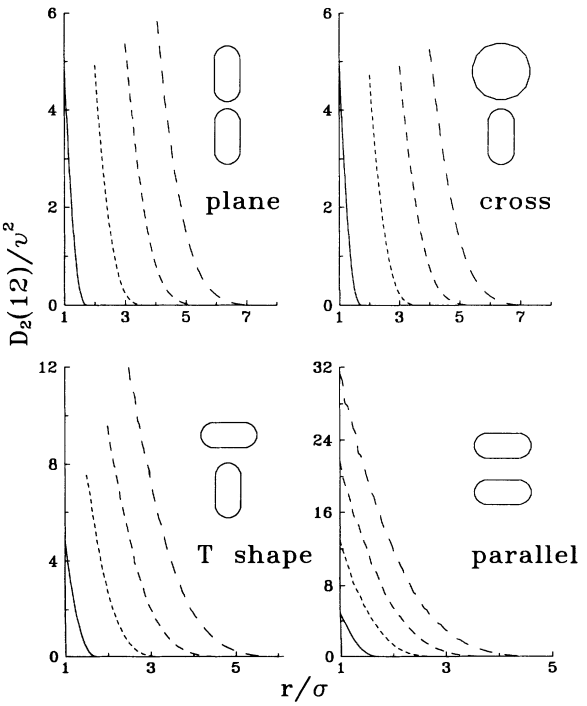

FIG. 3. $D_2(12)/v^2$ first bridge diagram reduced by the spherocylinder volume v for several orientations of the molecules 1 and 2. ——— hard spheres, - - - $l^* = 1$; – – – $l^* = 2$; — — — $l^* = 3$.

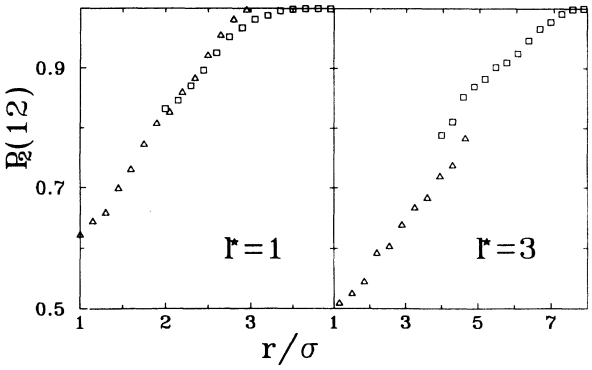

FIG. 4. $P_2(12) = D_2(12)/D_1^2(12)$ at $l^* = 1$ and 3. □ cross orientation, △ parallel orientation.

with hard sphere results. Overall r dependencies are similar to that of the hard sphere system. The contact values increase with increasing elongation and they strongly depend on θ_1 and θ_2. The ϕ dependence is less pronounced (compare the results for plane and cross orientations). Figure 4 shows the first bridge diagram divided by the first parallel diagram $P_2(12) = D_2(12)/D_1^2(12)$ for the cross and parallel orientations at $l^* = 1$ and 3. The results for the other orientations considered are similar; $P_2(12)$ is much less orientationally dependent than $D_2(12)$. In the PY and VM approximation $P_2(12) = 1$ and in the HNC approximation $P_2(12) = 0$. Thus, none of the closures considered is accurate in the low density region.

VI. CONCLUSIONS

We have performed Monte Carlo simulations of the structure and equation-of-state quantities of the HOS fluid using more particles and more configurations and for a larger spherocylinder core diameter than in a previous study [2].

We have compared the simulation data with the results of the PY, HNC, and VM integral equation theories. At low core diameters the VM spherical harmonic coefficients are in excellent agreement with the simulation results up to the highest packing fraction considered, $\eta = 0.45$. The PY and HNC results are slightly worse but still good. At the largest core diameter con-

TABLE I. The compressibility factors of the HOS. MC[a]—simulation results of Ref. [2], MC[b]—present simulation results, and EOS—equation of state of Ref. [7]. The PY, HNC, and VM values were obtained using the pressure equation (7).

η	MC[a]	MC[b]	EOS	PY	HNC	VM
			$l^*=1$			
0.05			1.25	1.25	1.25	1.25
0.10	1.58±0.01		1.58	1.58	1.58	1.58
0.15			2.02	2.00	2.06	2.01
0.20			2.59	2.54	2.70	2.57
0.25	3.35±0.07	3.35±0.01	3.36	3.25	3.60	3.33
0.30			4.40	4.18	4.87	4.35
0.35	5.79±0.07	5.81±0.02	5.81	5.41	6.68	5.75
0.40			7.79	7.04	9.32	7.69
0.45	10.53±0.07	10.53±0.03	10.60	9.25	13.23	10.43
			$l^*=2$			
0.05			1.29	1.29	1.30	1.29
0.10			1.69	1.68	1.70	1.68
0.15			2.21	2.18	2.27	2.20
0.20			2.91	2.85	3.05	2.89
0.25	3.83±0.05	3.85±0.01	3.84	3.71	4.14	3.81
0.30			5.09	4.84	5.65	5.06
0.35	6.79±0.05	6.81±0.02	6.79	6.33	7.76	6.74
0.40			9.11	8.32		9.06
0.45	12.30±0.10	12.39±0.04	12.37	11.02		12.26
			$l^*=3$			
0.05			1.34	1.34	1.34	1.34
0.10			1.80	1.80	1.83	1.80
0.15			2.43	2.40	2.51	2.42
0.20			3.27	3.20	3.45	3.25
0.25		4.39±0.01	4.38	4.24	4.74	4.37
0.30			5.77	5.61	6.50	5.86
0.35		7.80±0.02	7.82	7.42	8.93	7.86
0.40			10.45	9.84		10.54
0.45		14.30±0.07	14.07	13.10		14.15

TABLE II. The thermodynamic consistency of the PY, HNC, and VM approximations. Compressibility factors z_c calculated from the compressibility Eq. (8), $\Delta z = z_v - z_c$.

	PY		HNC		VM	
η	z_c	Δz	z_c	Δz	z_c	Δz
			$l^*=1$			
0.05	1.25	0.00	1.25	0.00	1.25	0.00
0.10	1.58	0.00	1.57	0.02	1.58	0.00
0.15	2.02	-0.02	1.98	0.08	2.02	-0.01
0.20	2.61	-0.07	2.50	0.20	2.60	-0.03
0.25	3.41	-0.16	3.16	0.44	3.37	-0.04
0.30	4.51	-0.33	4.00	0.87	4.41	-0.06
0.35	6.05	-0.64	5.08	1.60	5.82	-0.07
0.40	8.25	-1.21	6.49	2.83	7.77	-0.08
0.45	11.48	-2.23	8.37	4.86	10.50	-0.07
			$l^*=2$			
0.05	1.29	0.00	1.29	0.01	1.29	0.00
0.10	1.69	-0.01	1.69	0.01	1.69	-0.01
0.15	2.22	-0.04	2.22	0.05	2.22	-0.02
0.20	2.95	-0.10	2.93	0.12	2.93	-0.04
0.25	3.96	-0.25	3.85	0.29	3.89	-0.08
0.30	5.37	-0.53	4.99	0.66	5.18	-0.12
0.35	7.36	-1.03	6.28	1.48	6.93	-0.19
0.40	10.24	-1.92			9.33	-0.27
0.45	14.49	-3.47			12.64	-0.38
			$l^*=3$			
0.05	1.34	0.00	1.34	0.00	1.34	0.00
0.10	1.81	-0.01	1.81	0.02	1.81	-0.01
0.15	2.46	-0.06	2.46	0.05	2.45	-0.03
0.20	3.37	-0.17	3.33	0.12	3.33	-0.08
0.25	4.64	-0.40	4.46	0.28	4.50	-0.13
0.30	6.44	-0.83	5.85	0.65	6.09	-0.23
0.35	9.01	-1.59	7.35	1.58	8.23	-0.37
0.40	12.77	-2.93			11.10	-0.56
0.45	18.36	-5.26			14.99	-0.84

sidered ($l^* = 3$) and the largest packing fraction none of the theories describes $g_{000}(r)$ harmonic coefficient satisfactorily. The VM and PY reduced higher harmonic coefficients of the pair distribution function are in good agreement with the simulations even in this state point.

The equation-of-state results of the VM theory are very good, while the accuracy of the PY and HNC compressibility factors is poor at high densities. The same holds true for the thermodynamic consistency between the pressure and the compressibility equation.

We have also calculated a bridge diagram using Monte Carlo integration. It was shown that $D_2(12)$ strongly depends on the nonsphericity of molecules and on θ_1, θ_2 and that it depends much less on ϕ. It was also shown that none of the theories tested gives accurate results for the bridge function at low densities.

ACKNOWLEDGMENTS

The authors acknowledge support from the Grant Agency of the Czech Republic under Grant No. 203/93/2284.

[1] I. Nezbeda and T. Boublík, Czech. J. Phys. B **27**, 953 (1977); Mol. Phys. **51**, 1443 (1984); I. Nezbeda, Czech. J. Phys. B **35**, 752 (1985); W. R. Cooney, S. M. Thompson, and K. E. Gubbins, Mol. Phys. **66**, 1269 (1989).

[2] M. Wojcik and K. E. Gubbins, Mol. Phys. **53**, 397 (1984).

[3] S. Labík, A. Malijevský, and W. R. Smith, Mol. Phys. **73**, 87 (1991).

[4] S. Labík, A. Malijevský, and W. R. Smith, Mol. Phys. **73**, 495 (1991); R. Pospíšil, A. Malijevský, S. Labík, and W. R. Smith, *ibid.* **74**, 253 (1991); S. Labík, A. Malijevský, R. Pospíšil, and W. R. Smith, *ibid.* **74**, 261 (1991).

[5] R. Pospíšil, A. Malijevský, and W. R. Smith, Mol. Phys. **79**, 1101 (1993).

[6] S. Labík, R. Pospíšil, A. Malijevský, and W. R. Smith, J. Comput. Phys. (to be published).

[7] M. J. Maeso, J. R. Solana, and J. Amoros, Mol. Phys. **76**, 1269 (1992).